Natural gas displacement by wind curtailment utilization in combined-cycle power plants

Rao, A. Gangoli; van den Oudenalder, F. S.C.; Klein, S. A.

DOI
10.1016/j.energy.2018.11.119

Publication date
2019

Document Version
Final published version

Published in
Energy

Energy 168 (2019) 477–491

Contents lists available at ScienceDirect

Energy

journal homepage: www.elsevier.com/locate/energy

Natural gas displacement by wind curtailment utilization in combined-cycle power plants

A. Gangoli Rao [a, *], F.S.C. van den Oudenalder [a], S.A. Klein [b]

[a] Faculty of Aerospace Engineering, Delft University of Technology, Kluyverweg 1, 2629 HS, Delft, the Netherlands
[b] Process & Energy Laboratory, Delft University of Technology, Leeghwaterstraat 39, 2628 CB, Delft, the Netherlands

ARTICLE INFO

Article history:
Received 30 January 2018
Received in revised form
25 October 2018
Accepted 25 November 2018
Available online 28 November 2018

Keywords:
Combined-cycle
Curtailment utilization
Curtailment modelling
Thermal energy storage
Latent heat storage
Natural gas preheating

ABSTRACT

The energy scenario is currently undergoing a rapid transition in the pursuit of increasing the share of renewable energy sources in order to reduce the global anthropogenic CO2 emission. However, since several of the renewable energy sources are intermittent in nature, like wind and solar, this intermittency gives rise to several problems in energy production, distribution and management. A novel solution to store and utilize excess energy from intermittent renewable energy sources (IRES) in a combined cycle power plant (CCPP) is introduced. The overall thermal to electricity conversion efficiency of the proposed method is higher as compared to other contemporary energy storage solutions. The techno-economic feasibility analysis of the proposed method indicates that it can lead to annual fuel savings up to approximately 0.8%, thereby saving 3600 tonnes of CO2 emission annually for a typical power plant. The proposed concept paves the way to change the role of a combined-cycle power plant from being solely an energy provider to a contributor in energy storage and energy management.

1. Introduction

It has been proved beyond doubt that the human activity is driving the current climate change and geologists have named the current ongoing 6th great extinction called as Anthropocene [39] The European Union wants to be at the forefront of mitigating the climate change and therefore the twenty-seven member countries of the European Union have set targets to deliver 20% of their total energy generation solely from renewable energy sources by 2020.[1] Next to this target, a 20% reduction in greenhouse gases as compared to 1990 has been agreed upon. Because of these targets, the share of renewable energy within power generation has increased over the recent years[2,3]. With this development and cheaper electricity production cost, the share of intermittent renewable energy sources (IRES) such as wind power and solar energy will continue to increase significantly.

Due to the intermittent nature of renewable energy sources, integration challenges into the electrical grid is becoming a serious issue. One of these challenges is to maximize the utilization of renewable wind power by minimizing the “dispatch down time” of renewable power, also known as curtailment. There are several reasons for curtailment, such as lack of transmission availability, system balancing challenges and system stability [6]. The usage of the term ‘curtailment’ broadly refers to the use of less wind or solar power that is potentially available at a given time. Definitions of curtailment can vary, and the availability and tracking of curtailment are limited in some areas [4]

The loss from curtailing renewable energy generation is generally seen as an unacceptable solution by the public. The main argument is that it is a loss of green energy and an economic loss to curtail generation with near zero marginal costs [14] On the other hand, the society also demands a high degree of energy security, which is defined as the reliable and uninterrupted supply of energy that is sufficient to meet the needs of the economy and is at the same time, reasonably priced [16]. According to the European Directive 2009/28/EC, renewable energy systems (RES) enjoy preferential treatment in the electricity grid as far as the secure operation of the power system is not compromised [34] Already today, more frequent occurrences of curtailment for renewable generators are observed in areas with high shares of renewables

* Corresponding author.
E-mail address: A.Gangolirao@tudelft.nl (A.G. Rao).

[1] European Union Committee, 2008. The EUs Target for Renewable Energy 20% by 2020. Report.

[2] International Energy Agency, 2015. Recent Energy Trends in OECD, Excerpt from: Energy Balances of OECD Countries. Report.

[3] International Energy Agency, 2015. World Energy Trends, Excerpt from: Energy Balances of Non-OECD Countries. Report.

https://doi.org/10.1016/j.energy.2018.11.119

Nomenclature

Latin Symbols

C_F	Annual fuel Savings
C_I	Investment cost
C_M	Maintenance cost
C_P	Specific heat
C_{CB}	Annual carbon allowance savings
C_{total}	Total cost
d_i	Inner diameter
$E_{generated}$	Total generated energy
H	Enthalpy
h_{st}	Latent heat of fusion
K	Thermal conductivity
L	Length
Nu	Nusselt number
$Nu_{laminar}$	Nusselt number for laminar flow
$Nu_{turbulent}$	Nusselt number for turbulent flow
P_D	Power demand
Pr	Prandtl number
R	Radial coordinate
r_a	Upper radial coordinate of control volume element
r_b	Lower radial coordinate of control volume element
r_i	Inner radius
r_o	Outer radius
Re	Reynolds number
$SNSP_{limit}$	SNSP limit threshold value
T	Temperature
t	Time
T_m	Melting temperature
T_∞	Heat transfer fluid stream temperature
$T_{surface}$	Surface Temperature
TCG_{limit}	TCG limit threshold value
U	Heat transfer coefficient
Z	Axial coordinate

Greek symbols

ΔE	Energy difference
Δt	Time step
Δz	Axial coordinate step
λ	EUR per kg of CO_2 reduced
μ	Dynamic viscosity
Ø	Angular coordinate
ρ	Density
τ	Lifetime
ε	Intermediate value used for Nusselt number computation

Superscripts

t	Index for current time

Subscripts

Boundary	Boundary between HTF and PCM
CCPP	Combined-cycle power plant
HTF	Heat transfer fluid
I	Index for nodes in r-direction
J	Index for nodes in z-direction
PCM	Phase change material
TES	Thermal energy storage
WT	Wind turbine

Abbreviations

CCPP	Combined-cycle power plant
CHP	Combined heat and power
ETS	European trading system
EU	European Union
FDM	Finite difference method
HP	High pressure
HTF	Heat transfer fluid
IRES	Intermittent renewable energy source
LP	Low pressure
MP	Medium pressure
PBP	Payback period
PCM	Phase change material
SNSP	System non-synchronous penetration
TCG	Transmission control group
TES	Thermal energy storage

[11] Since 2010 China has faced a worrying “wind curtailment” in the development and operation of the wind power industry. This has resulted in a sharp decline of the utilization hours of the wind power, seriously affected the economic benefits of the wind farms and caused serious energy waste [24]

Integration of renewable energy leads to increased costs of the entire electric system [28]. show that the cost of electric storage ($/kWhr) increases substantially with % of wind curtailment. Curtailment cost inclusion in their model adds anywhere from 10% to 60% to the value provided by infrastructure investments in storage and dispatchable loads. The proportion provided from the curtailment cost is higher with higher wind penetration levels. [38]; state that at a high wind energy penetration, integration costs can be in the same range as generation costs of wind power and conventional plants. As an example, since 2010, system operation costs have increased by 62% in Britain [15] Andoni et al. [43] studied the properties of several curtailment rules widely used in UK renewable energy projects and their effect on the viability of renewable generation investment using Game-Theory modelling. It should be noted that inadequate management of the grid when integrating intermittent renewable energy sources can lead to black-outs [17]

The total installed wind power capacity worldwide by the end of 2017 was 539.6 GW, which is 11% increase when compared to 2016.[4] Several solutions have been proposed to reduce wind energy curtailment, each trying to solve a different aspect. The most promising method is to use large-scale energy storage systems to store energy during periods of low demand and release it during periods of high demand [1–3,20,29,31] [40]; Denholm & Mai (2019) looked into the timescales of the energy storage required for reducing curtailment in Texas and concluded that when 8.5 GW of storage capacity with 4 h of duration is added to the system, the curtailment of renewable energy can be reduced to 8%–10%. However many storage solutions are expensive and the efficiency of energy storage and reconversion to electricity is not high. Recent efforts have also been focused on using excess wind power for district heating to displace fossil fuels [23,30] Another solution is to adjust the power demand pattern to better match the power supply by having a variable electricity price based on the time of day or availability of renewable energy sources. [36]; looked at changing people's behaviour in relation to energy consumption and analysed

[4] Energy GW. Global wind statistics 2017. Global Wind Energy Council; 2017.

determinants behind an individual's decision to adopt curtailment behaviour [32]. propose a scenario-based planning framework for energy storage systems with the main goal of mitigating wind curtailment issue.

2. Proposed methodology

A novel solution for the utilization of excess wind power is proposed in this paper. Currently, a power plant is mainly used as a generator of electricity and not as a consumer. Instead of powering the plant solely by burning fossil fuels, one can (partly) power it with the excess power obtained from IRES. Allowing the plant to extract power from the grid can lead to a displacement of fossil fuels to some extent. The concept proposes to preheat natural gas used in combined-cycle power plants (CCPPs) using the otherwise curtailed wind power. This would increase the sensible enthalpy of the fuel and would thereby reduce the fuel consumption of the power plant. Thus, this solution has the potential to partly power the power plant with stored excess energy produced by IRES, thereby decreasing its fuel consumption and greenhouse gas emissions. By doing so, power plants no longer solely balance the grid by adjusting the power supply, but also by influencing the demand. This new way of balancing the IRES has not yet been looked into and this is the first paper to propose this novel solution and to investigate its feasibility.

The basics of the methodology are:

- During the period of curtailment (high wind production compared to the demand), the excess wind power is stored as thermal energy.
- During 'normal' periods, the stored thermal energy is used to preheat the natural gas used to fuel the gas turbine in a combined cycle power plant (a maximum technical achievable temperature of 165 °C is assumed such that the change in the fuel Wobbe index is less than 5%).

The stored thermal energy could also be used to preheat the compressed air in a gas turbine before entering into the combustion chamber, however, this would be a complex system and would require substantial changes in the engine architecture and the powerplant architecture. Therefore, it was chosen to preheat the natural gas and not the compressed air to minimize the impact on the design of the standard gas turbine design and operation. A schematic of the proposed methodology with respect to the conventional approach is shown in Fig. 1.

The research objective of this paper is to assess the technical and financial feasibility of storing thermal heat during periods of excess power production and by using this stored heat to preheat natural gas at a later stage during periods with net power demand.

This objective is achieved by the development and the usage of three mathematical models. The first model simulates the occurrence and quantity of wind curtailment. The second model simulates the part-load and annual performance of a combined-cycle power plant. The third model simulates a thermal storage system used to store the excess wind power. The combination of these models simulates the annual effects of using wind curtailment utilization in an operational CCPP within the Dutch electricity grid and power market.

3. Curtailment model

An important aspect of the feasibility analysis is to determine the quantity of curtailment of wind power that can be prevented by the proposed concept. Therefore the frequency of occurrence and the quantity of curtailment should be calculated. This was performed based on the methodology explained by McKenna et al. [26], in which the authors present a simplified model to estimate the occurrence of curtailment in an isolated grid system.

Fig. 2a displays an illustrative period throughout the year 2015 to demonstrate how the occurrence of curtailment can be estimated. It displays the national power demand for The Netherlands and two grid stability limits as defined in the McKenna paper. The first stability limit deals with frequency control requirements and is referred to as the system non-synchronous penetration (SNSP) limit. It sets a threshold above which nonsynchronous sources are not allowed into the grid due to system stability reasons [25,26]. This limit is computed by means of eqn. (1). A limit of 100% represents a grid which can be fully operational with solely nonsynchronous generation sources.

For reasons of simplicity, no national power imports or exports are considered in the current study.

$$\mathrm{SNSP}_{\mathrm{limit}} = \frac{P_{WT} + Imports}{P_D + Exports} \tag{1}$$

The second grid stability limit in McKenna is referred to as the regulating and reserve limit (RR) limit [25,26]. It states that a group of thermal generators must be in operation as a spinning reserve to adjust their power in response to unplanned changes in power demand and/or supply. Therefore, a minimum number of thermal power plants must constantly be in operation. For simplicity, this minimum power generation was taken to be constant throughout the year and was defined as a percentage of the maximum annual demand, as shown in eqn. (2). A limit of 100% indicates that the complete grid demand must always be delivered by thermal generators.

$$\mathrm{TCG}_{\mathrm{limit}} = \mathrm{X} \cdot \mathrm{P}_{\mathrm{D,max}} \quad (0 \leq \mathrm{X} \leq 1) \tag{2}$$

Using the national demand with SNSP limit of 60% (eqn. (1)) and a regulating and reserve limit (RR) of 20% (eqn. (2)), the maximum allowable amount of renewables (wind and solar) can be calculated. This is visualized in Fig. 2b as allowable wind power for a typical period of one week. This figure also includes a typical wind generation pattern based on the assumption that 30% of the annual power demand is generated by wind. It can be observed that occasionally more wind power is present than allowed, this is classified as an excess of wind power. For the illustrative period, the resulting curtailment is shown in Fig. 2c. Grid stability requirements limit the minimum thermal generation and thereby reduce the available capacity left for wind power.

This simplified curtailment model is used in the remainder of this paper to estimate the impact of wind penetration on the occurrence and quantity of curtailment. It should be noted that the focus of the paper is not on establishing an accurate wind curtailment model but to rather use a simple system to perform the technical and economic feasibility of the proposed concept. The difference between a conventional system and the proposed system is shown in Fig. 1.

4. Combined-cycle power plant model

To evaluate the effect of the proposed solution on a realistic combined-cycle power plant, an accurate model of a combined-cycle power plant is required. A set of criteria were first established to select a suitable power plant, as described below.

4.1. Power plant selection

Several criteria were established to select a suitable power plant for modelling purposes. The main criteria considered are as follows:

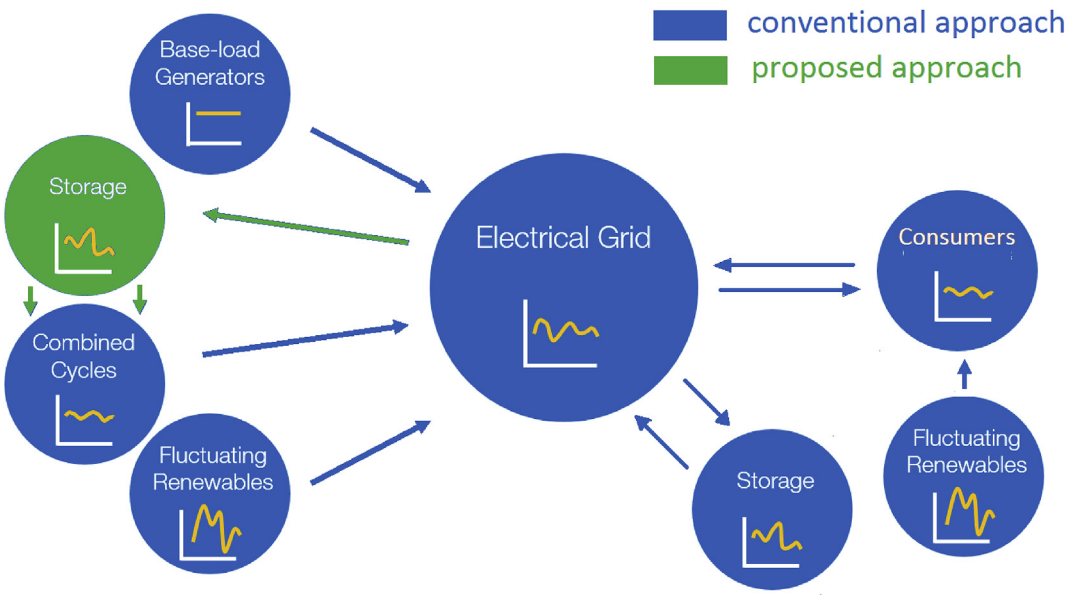

Fig. 1. Schematic of the conventional approach and proposed approach to energy management.

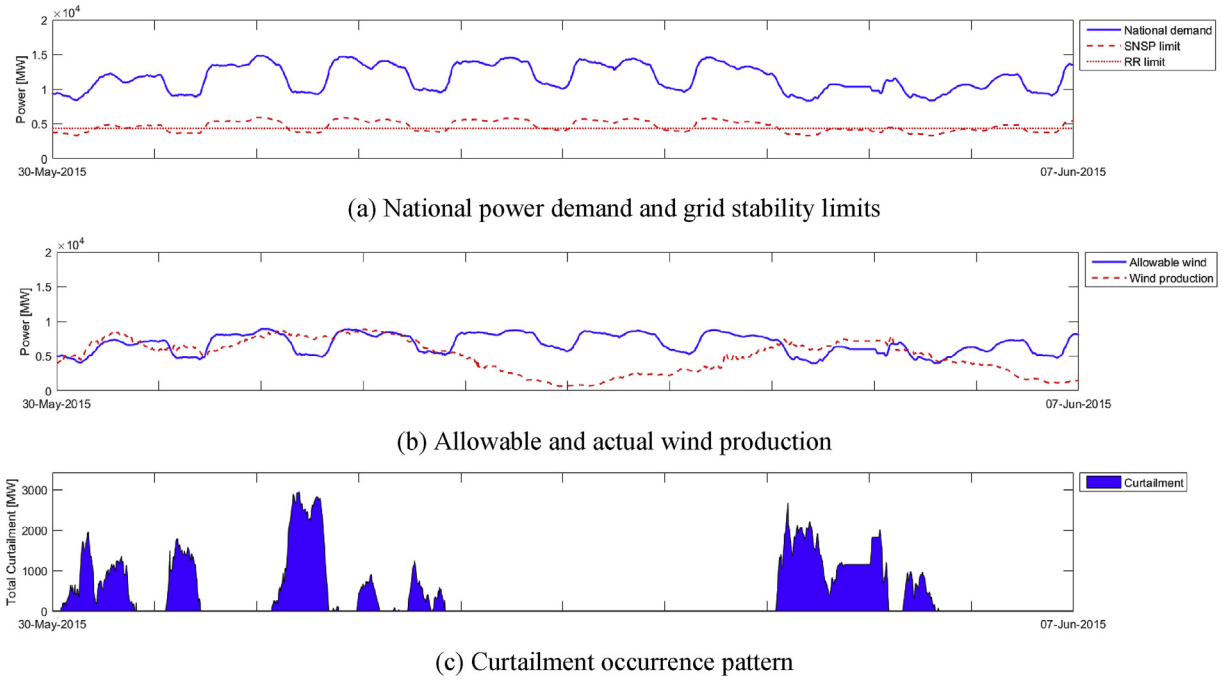

Fig. 2. Wind curtailment simulation method for the Dutch electrical grid at 30% wind penetration and 60% system non-synchronous penetration (SNSP) and 20% (regulating and reserve) RR limits.

- The power plant is only used for power generation
- The power plant should be a state of the art combined-cycle power plant
- The operating pattern and component data should be available for accurate modelling of the power plant

After several deliberations, the Hemweg 9 power plant in Amsterdam,[5] The Netherlands, was selected as it fulfils all of the above-mentioned criteria. The Hemweg 9 power plant became operative in 2012 and is used solely to produce electricity. It has a maximum power output of 440 MWe, which is representative of modern combined cycle power plants in Europe. During the writing of this article, no known major policies were in effect restricting its operation, thus making it a good benchmark. It consists of a single shaft configuration and uses a three-pressure stage heat recovery steam generator (HRSG). The gas turbine, steam turbine and generator are all supplied by Siemens: a Siemens SGT5-4000F gas

[5] https://powerplants.vattenfall.com/en/hemweg-9.

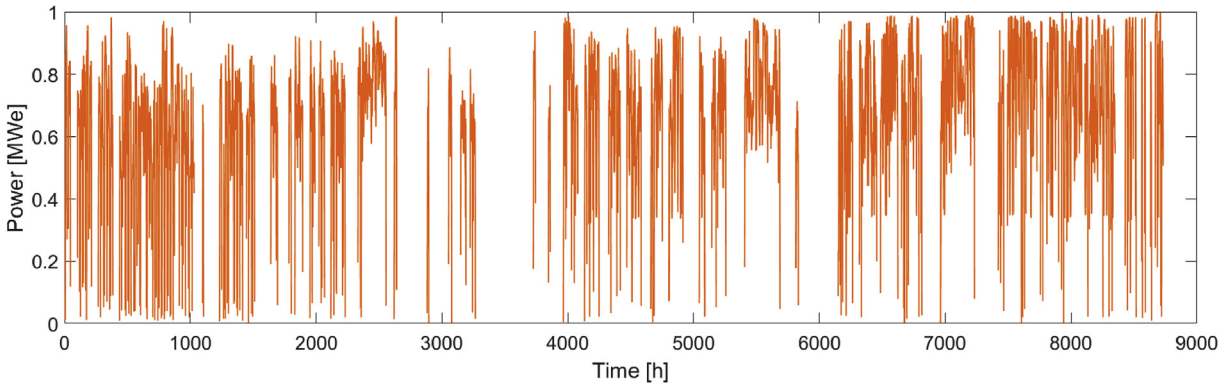

Fig. 3. The normalized operating pattern for the Hemweg 9 for 2015[9].

turbine, an SST-5000 steam turbine and an SGen5-2000h hydrogen-cooled generator[6,7,8]. The operating pattern for the Hemweg 9 during the year 2015 as shown in Fig. 3.

4.2. Combined cycle power plant model

The CCPP was modelled using THERMOFLEX®, developed by the Thermoflow®. It allows the user to model the design and off-design performance of various power plants, including CCPP architectures. In the model, gas turbine flue gases are divided into two streams, one of which enters the high pressure (HP) superheater, where the steam is superheated. The other stream passes through the reheater. After partial expansion through the HP turbine, the steam is reheated before entering the medium pressure (MP) turbine. After the steam is expanded through the MP turbine, it is mixed with steam coming from the LP superheater before entering into the low pressure (LP) turbine. The condenser at the exit of the LP turbine is water cooled. All publicly known data from Siemens® was implemented using their specification reports. The HRSG design specifications were based on a similar reference plant whose main characteristics are presented in Table 1. Economisers, evaporators, superheaters and reheaters are modelled as heat exchangers (specifications are presented in Table 1). For comparison, an identical model is developed and evaluated using Cycle-Tempo®. The Cycle-Tempo® has been developed by the Delft University of Technology in collaboration with Nederlandse Organisatie voor toegepast-natuurwetenschappelijk onderzoek (TNO). It is used to evaluate the thermodynamic behaviour of energy systems. The simulation results for both models can be found in Fig. 4.

4.3. Results from the CCPP model

The plant performance at part-load conditions is displayed in Fig. 4a and b. It can be seen that at high loads, the Cycle-Tempo model estimates slightly higher efficiencies than the model created in THERMOFLEX. The main reason for the deviation between the two models is mainly due to differences in the modelling of the gas turbine component maps. Nevertheless, it can be observed that both models predict a similar trend in their operation.

Table 1
Power plant HRSG specifications.[10]

Parameter	Value	Unit
Design gross power	427	[MWe]
Heat recovery steam generator		
HP steam temperature	565	[°C]
HP steam pressure	125	[bar]
HP evaporator pinch point	15	[°C]
MP steam temperature	565	[°C]
MP steam pressure	30	[bar]
MP evaporator pinch point	12	[°C]
LP steam temperature	300	[°C]
LP steam pressure	5	[bar]
LP evaporator pinch point	20	[°C]
Waterside pressure drop	1	[%]
Gas side pressure drop (evaporators)	1	[mbar]
Gas side pressure drop (other)	4	[mbar]

The validation of the steady-state model was performed by comparing the results to those found in the literature [5,18]. It must be noted that the exact model architectures evaluated in the literature are unknown. As shown in Fig. 4a and b, both THERMOFLEX and Cycle-Tempo underestimate plant performance compared to values provided in the literature. However, since all the modelling parameters and assumptions used for modelling the power plant described by Refs. [18] are not known, some discrepancy within the model is expected. From Fig. 5 it can be said that the created power plant models are sufficient to provide a good estimation of CCPP performance.

These curves together with publicly available data for 2015[11] on the hourly production of the Hemweg 9 allow computing the annual performance displayed in Table 2. This annual performance serves as a baseline case without curtailment utilization. It must be noted that to obtain the power plant's annual performance, steady-state performance curves were used, transient behaviour (such as ramp-ups and shutdowns) were not included.

Using the above-mentioned model, the operating characteristics of the Hemweg 9 power plant has been computed and shown in Fig. 5. A quick inspection indicates that the plant often operates at off-design conditions and therefore at lower thermal efficiency. The computed average gross thermal efficiency for 2015 was 55.11%.

[6] Siemens AG, 2008. Siemens Gas Turbine SGT5-4000F. Report.
[7] Siemens AG, 2010. Siemens Steam Turbine SST-5000 Series. Report.
[8] Siemens AG, 2013. The Hydrogen-Cooled SGen-2000H Generator Series. Report.
[9] ENTSO-E, \Actual Generation per Generation Unit." Available at. https://transparency.entsoe.eu/generation/r2/actualGenerationPerGenerationUnit/". Accessed online: 27-04-2016.
[10] Siemens AG, 2009. SCC5-4000F (SST5-5000) for cold climate conditions. [ONLINE] Available at: http://www.slideshare.net/siemens_answers/power-generation-power-plants. [Accessed 05-01-2016].
[11] Available from https://transparency.entsoe.eu.

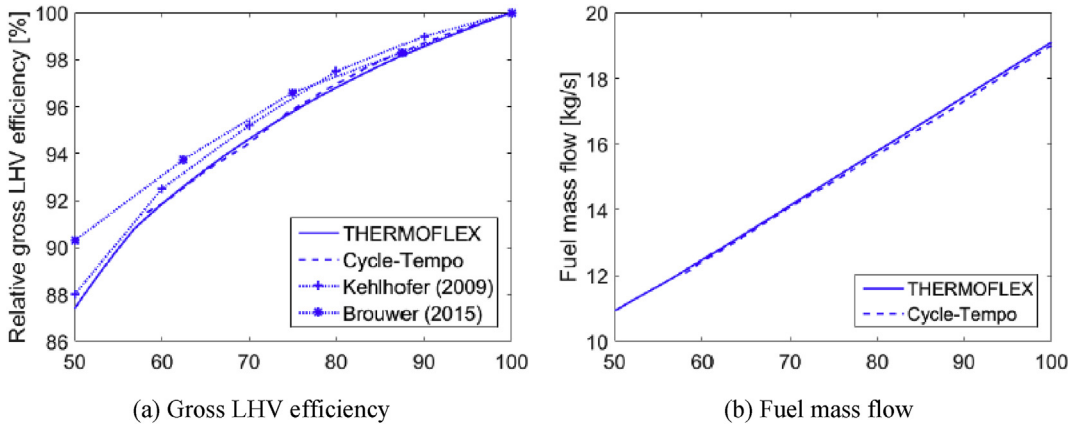

Fig. 4. Combined-cycle off-design performance at ISO conditions [5,18].

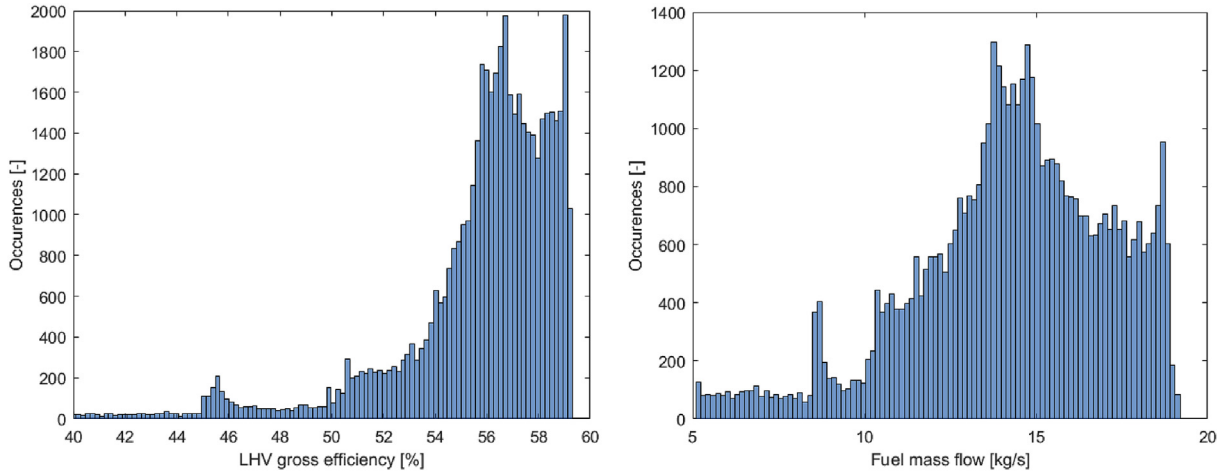

Fig. 5. Annual occurrence distribution for the gross thermal efficiency and fuel mass flow rate for the Hemweg 9 powerplant.

Table 2
Annual performance of the reference power plant.

Parameter	Value	Unit
Energy generated	1,257,234	[MWh]
Operating hours	4220	[hour]
Average gross efficiency	55.11	[%]
Natural gas consumption	212,030	[tonne]
Air consumption	8,278,198	[tonne]
CO_2 emitted	451,191	[tonne]

5. Thermal storage model

A thermal storage system is selected and designed to store energy when there is excess wind power available and to release the heat to preheat the gaseous fuel used for CCPP when there is no curtailment. The section and design process is explained in the subsequent subsections.

5.1. Storage method

Various storage technologies were evaluated based on their techno-economic performance [3,7,8]. It was found that no single technology meets all the requirements for a perfect storage system [7]. Thermal energy storage (TES) has a suitable storage duration from several minutes up to several months and is relatively inexpensive per kWh, as is visible in Fig. 6. Within TES, the use of latent heat storage is preferred due to its constant recovery temperature and simpler technology [9]. During a heat storage cycle starting from a lower temperature, the thermal energy increases the temperature of the PCM (sensible enthalpy), subsequently the thermal energy is stored in the form of latent enthalpy when the temperature reaches the PCM melting point and the phase change occurs. Thus, the total energy is stored in the form of latent and sensible heat.

5.2. Storage module layout

The thermal storage consists of several identical modules in parallel. Each module consisting of a hollow cylinder in which the natural gas is surrounded by a PCM. Within the cylinder, heat is exchanged between the PCM and the natural gas, also known as the heat transfer fluid (HTF). The HTF enters the cylinder at $z = 0$ at its initial temperature and leaves the cylinder at $z = L$ at elevated temperature. To heat the PCM, two electrical heating elements are used, as visualized in Fig. 7. The first element is located at the inner radius (ri) to directly heat the HTF when the CCPP is online. The second heating element is located at the outer radius (ro) to heat the PCM when the CCPP is offline and there is no flow of natural gas (the HTF has zero velocity). The optimum dimensions of the inner radius, outer radius and length are to be determined at a later stage

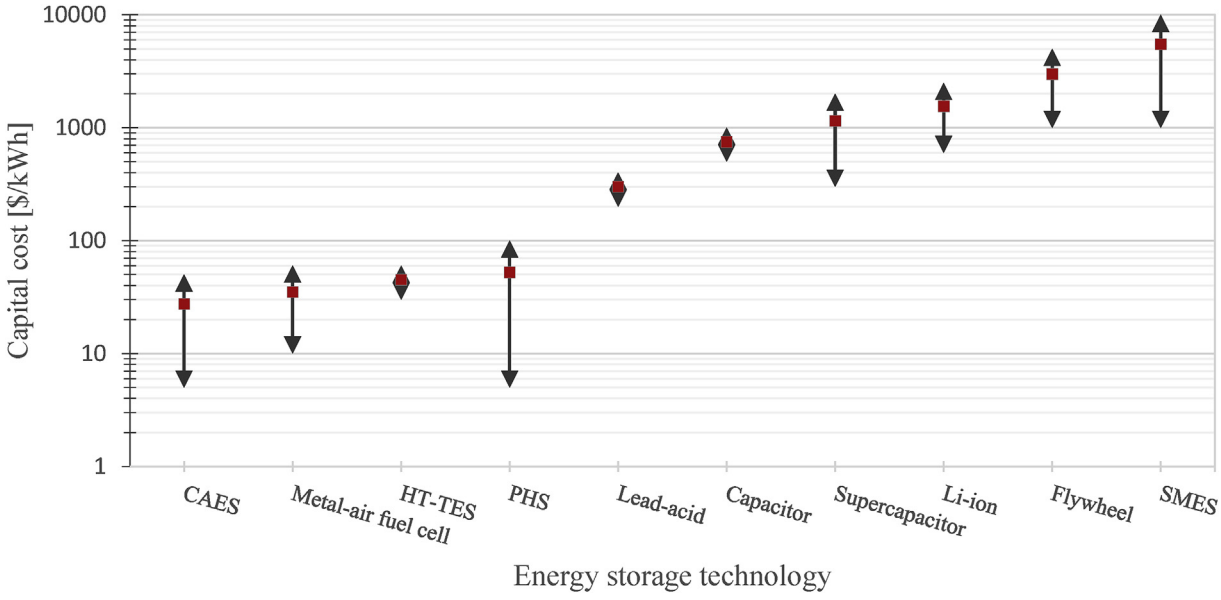

Fig. 6. Energy storage technologies cost per kWh. Based on [7].

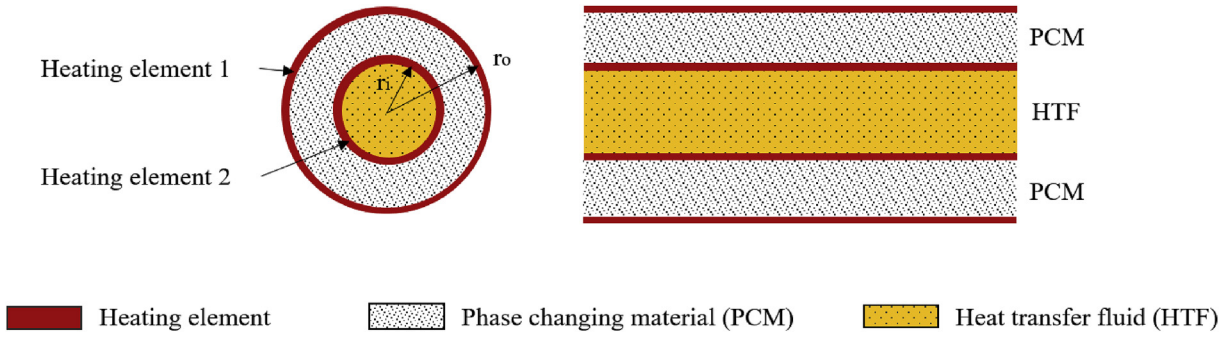

Fig. 7. Thermal storage module geometry. Front view (left) and side view (right).

by means of modelling the performance of the thermal storage model. Unless stated otherwise, the outer radius ro is assumed to be twice the size of the inner radius ri.

5.3. The PCM selection

A suitable PCM is chosen according to three main criteria mentioned in the literature [10,12,37,41], the phase change temperature, latent heat of fusion, and PCM density. To preheat the natural gas to a maximum of 165 °C, a suitable candidate should have a phase change temperature slightly above this temperature. From a latent heat point of view, it is beneficial to have a high latent heat of fusion to maximize the latent heat released and stored during operation. From the PCM's density point of view, higher density is preferred as this leads to a smaller required volume for a given amount of PCM mass. By evaluating these three criteria for the candidates as shown in Table 3, it was concluded that the PCM "A164" has the most suitable properties for the considered application. A164 is a commercial organic PCM solution produced by the Phase Change Material Products Limited.[12] Its characteristics are presented in Table 4.

[12] Phase Change Material Products Limited. 2016. [ONLINE] Available at: http://www.pcmproducts.net [Accessed 14-05-2016].

5.4. The numerical model

To optimize the design of the thermal storage and the gas heating system as described earlier, a numerical model is created based on the fundamentals of heat transfer. This numerical model is later used to design, analyse and optimize the system presented in the earlier subsection.

The main assumptions in the numerical model are summarized below.

General assumptions.

- Radiation heat transfer is negligible
- Heat losses to the ambient are negligible
- The HTF flow is fully developed within the cylinder
- The thermophysical properties are independent of temperature

Assumptions for the phase changing material.

- There is no supercooling and hysteresis
- It is homogeneous and isotropic
- Volume change during phase change is negligible
- Heat transfer within the PCM is assumed to be controlled by conduction

Table 3
Phase change material candidates [12,19,33].

Name	Phase change temp. [°C]	Latent heat of fusion [kJ/kg]	Density [kg/m^3]
Salicylic acid	159	199	1443
Benzanilide	161	162	–
A164	164	306	1500
O-mannitol	166	294	1489
Hydroquinone	172	258	1358
Pentaerythritol	187	255	–
$LiNO_3$-$NaNO_3$	195	252	–

Table 4
A164 characteristics .[10]

Parameter	Value	Unit
Melting temperature	164	[°C]
Latent heat of fusion	306	[kJ/kg]
Density (liquid phase)	1500	[kg/m3]
Density (solid phase)	1710	[kg/m3]
Thermal conductivity (liquid phase)	0.53	[W/m K]
Thermal conductivity (solid phase)	1.09	[W/m K]
Specific heat (liquid phase)	1800	[J/kg K]
Specific heat (solid phase)	2400	[J/kg K]

The 3-D heat diffusion equation in cylindrical coordinates is shown in eqn. (3). The heat transfer to the HTF is described by Eqn. (4) [21,35]. In this equation, the heat transfer coefficient is referred to as *U*.

$$\rho \cdot C_P \frac{\partial T}{\partial t} = \frac{1}{r}\frac{\partial}{\partial r}\left(k \cdot r \frac{\partial T}{\partial r}\right) + \frac{1}{r^2}\frac{\partial}{\partial \varphi}\left(k\frac{\partial T}{\partial \varphi}\right) + \frac{\partial}{\partial z}\left(k\frac{\partial T}{\partial z}\right) \tag{3}$$

$$\frac{\partial T}{\partial t} = -\frac{2U}{\rho \cdot C_P \cdot r_i}\left(T_{HTF} - T_{surface}\right) \tag{4}$$

Based on the assumption that the problem is axisymmetric, the 3-D diffusion equation can be simplified to a 2-D problem.

A finite difference method (FDM) is used (forward in time and central in space) to solve this transient problem. This technique replaces partial derivatives by suitable approximations based on a nodal network. This network consists of several nodes and for each of these nodes, the temperature is computed at each time step. The boundary conditions are represented by eqn. (5) to eqn. (7). The boundary node expressions were derived using the ghost node approach (shown in Fig. 8), at $r = r_0$

$$\left(k\frac{\partial T}{\partial r}\right) = 0 \tag{5}$$

at $r = r_i$

$$\left(k\frac{\partial T}{\partial r}\right) = U\left(T_{surface} - T_{\infty}\right) \tag{6}$$

at $z = 0$ and $z = L$

$$\left(k\frac{\partial T}{\partial z}\right) = 0 \tag{7}$$

The PCM's latent heat of fusion is accounted for via the enthalpy method [27]. This method is deemed to be the most efficient when using a fixed-grid approach [22]. The enthalpy is a temperature-dependent variable and is used to compute the latent heat flow through the PCM. To account for this, the node expressions are rewritten to include their enthalpy at the relevant node rather than temperature. The new enthalpy at the time t = t + 1 is then related to temperature change by means of the temperature-enthalpy relation given by eqn. (8).

$$h(T) = \begin{cases} C_{P,solid}(T - T_m) & for\ T < T_m \\ C_{P,solid}(T_m + h_{sl}) & for\ T = T_m \\ C_{P,liquid}(T - T_m) + h_{sl} & for\ T > T_m \end{cases} \tag{8}$$

To simulate the movement of the HTF at each specific time, the temperature of each node is transferred to its neighbouring node. This is allowed since forced convection is present [27]. To assure that the time step corresponds to the distance Δz travelled, it is expressed as follows:

$$\Delta t = \frac{\rho \pi r_i^2 \Delta Z}{\dot{m}} \tag{9}$$

This equation is based on the assumption that the density of the HTF does not change appreciably with temperature. The heat transfer coefficient is computed using the Reynolds and Prandtl numbers, shown by eqns. (10) and (11) respectively.

$$Re_{di} = \frac{\rho \cdot V \cdot d_i}{\mu} \tag{10}$$

$$Pr = \frac{\mu \cdot C_P}{k} \tag{11}$$

Based on these flow characteristics, the Nusselt number is computed using the appropriate equation for the flow regime, eqn. (12) for laminar and eqn. (13) for turbulent flow[13].

$$Nu_{laminar} = 3.66 + \frac{0.65\, Re_{di} \cdot Pr \frac{d_i}{L}}{1 + 0.04\left(Re_{di} \cdot Pr \frac{d_i}{L}\right)^{2/3}} \tag{12}$$

$$Nu_{turbulent} = \frac{\left(\frac{\varepsilon}{8}\right) Re_{di} \cdot Pr}{1 + 12.7\sqrt{\frac{\varepsilon}{8}}\left(Pr^{\frac{2}{3}} - 1\right)}\left[1 + (d_i/L)^{2/3}\right] \tag{13}$$

where:

$$\varepsilon = (1.8\, log_{10} Re_{di} - 1.5)^{-2} \tag{14}$$

Finally, the heat transfer coefficient can be computed via the Nusselt number by means of eqn. (15).

[13] Gorenflo, D., 1993. VDI Heat Atlas. Springer.

[14] Centraal Bureau voor de Statistiek. 2016. *Elektriciteitsbalans; aanbod en verbruik. [ONLINE] Available at:* http://statline.cbs.nl/statweb/publication/?dm=slnl&pa=00377. [Accessed 04-01-2016].

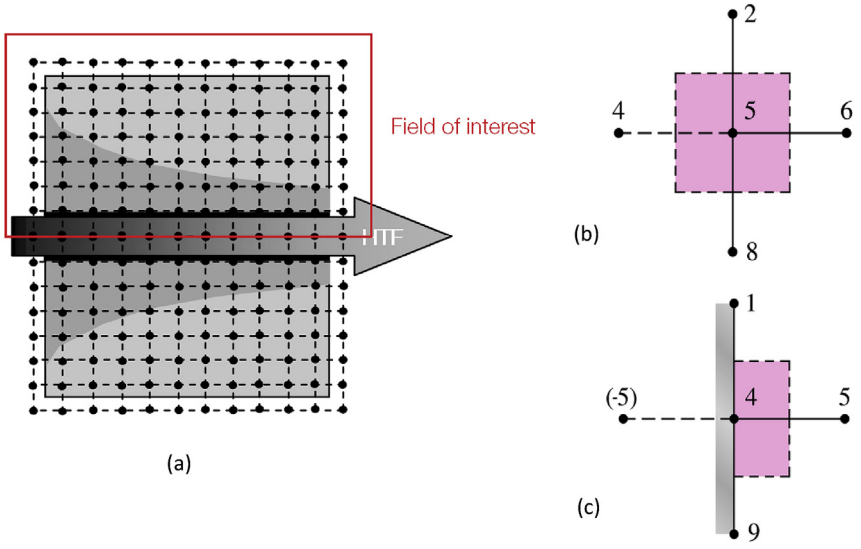

Fig. 8. (a) Generic mesh for PCM and HTF temperature field simulation in a hollow cylinder. (b) Interior node (c) boundary node.

$$U = \frac{N_u \cdot k}{d_i} \tag{15}$$

5.5. Grid convergence

A grid independence study was carried out by increasing the grid density gradually until the point when results did not vary significantly with any further increase in the grid density, as shown in Fig. 9. The HTF exhaust profile was used as the monitoring parameter. The solution converged at a grid size of 101×21 (number of nodes in axial direction times radial direction) since its temperature profile did not differ significantly from the 161×61 grid temperature profile. The deviation between these two grid densities in terms of the temperature at $t = 1 \times 10^5$ s was found to be 0.02%. This deviation is deemed as acceptable and further computations are performed with a 101×21 grid density, unless the module dimensions were changed. For these cases, a new grid independence study was performed.

5.6. Model verification

Model verification was performed by computing the energy balance at each time step and also at the end of the simulated time period. All energy transferred to the HTF must be equal the energy lost in the PCM. In addition, these quantities of energy must be equal to the energy passing through the boundary between HTF and PCM. These three quantities were independently computed as follows:

$$\Delta E_{HTF} = \rho \cdot C_P \pi r_i^2 \Delta z \int_0^t \sum_{j=1}^{M} \left(T_{HTF}^{t+1} - T_{HTF}^{t} \right) dt \tag{16}$$

$$\Delta E_{Boundary} = 2\pi r_i \Delta z \int_0^t \sum_{j=1}^{M} \left(T_{surface}^{t} - T_{HTF}^{t} \right) dt \tag{17}$$

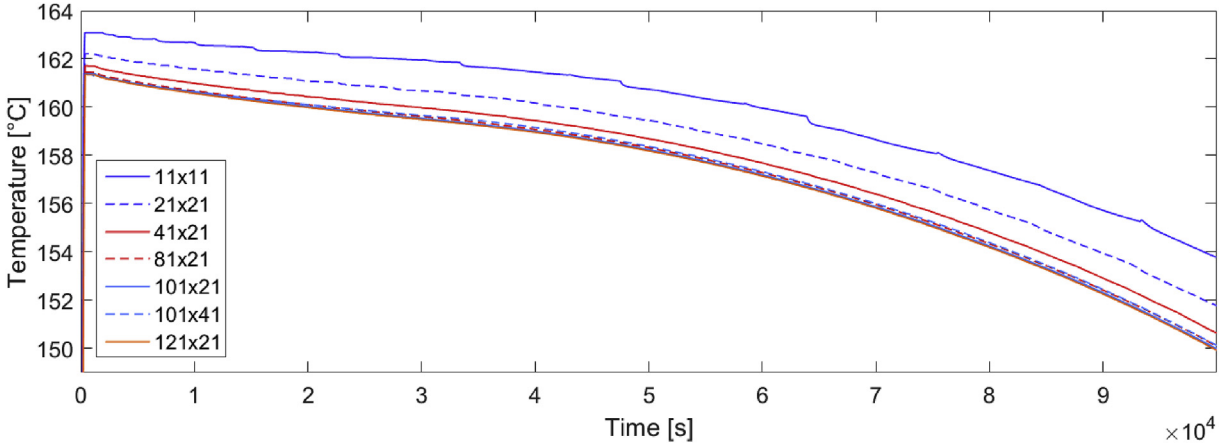

Fig. 9. Influence of grid density on the heat transfer fluid exhaust temperature profile (number of nodes in r-direction times the number of nodes in the z-direction).

$$\Delta E_{PCM} = \rho_{PCM} \cdot \pi \cdot z\left(r_a^2 - r_b^2\right) \int_0^t \sum_{i=1}^{N} \sum_{j=1}^{M} \left(h_{i,j}^{t+1} - h_{i,j}^{t}\right) dt \qquad (18)$$

The energy balance is checked, the maximum absolute deviation in the energy balance was found to be 0.045%, less than 1% as recommended [21,42].

5.7. Validation

To validate the above-described model, a specific test case based on two articles reported in the literature was used [13,35]. A shell-and-tube heat storage module was simulated in which a cold PCM was heated by a warmer HTF. The exact details of the simulation have been presented by researchers [13]. The only difference between both simulations was the time step used for the simulations, a time step of 0.001 s was used in the current simulations rather than the 2 s used in the literature. The HTF exit temperature is visualized and compared to the results found in the literature in Fig. 10. Thus, it can be said that the heat transfer model created is validated and can be used to analyse the problem.

6. Performance evaluation of the concept on an annual basis

To evaluate the performance of the proposed concept in terms of fuel savings and CO_2 emissions, it is compared to the performance of a combined-cycle power plant operating without the proposed fuel gas preheating system. This analysis is performed on an annual basis, based on publicly available data for the Hemweg 9 power plant and the national electricity demand for the Dutch market in 2015.

6.1. Integration of models

The model integration is executed as documented in the N2 chart shown in Fig. 11. The annual curtailment pattern together with the annual operating pattern of the power plant is used to perform a simulation for calculating the fuel temperature. The curtailment pattern determines when the storage is charged and the plant operating pattern determines when it is discharged. This simulation is performed for a full year. The output of the energy storage model is an annual pattern for the natural gas temperature which enters the power plant. Using this pattern and the simulated performance curves, as presented earlier, the annual fuel consumption can be computed.

Using all the three previously described models, the annual fuel consumption for the CCPP with curtailment utilization was computed for the year 2015. This has been performed using the storage dimensions and curtailment scenarios presented in Table 5. To assess how the outcome changes for different curtailment levels and storage sizes, a sensitivity study is performed for optimizing the module length and inner radius. To ensure that the outcome from the numerical simulations is grid independent, a new grid convergence study was performed.

The thermal storage operates in four different modes, as shown in Fig. 12. Its operational mode depends on whether curtailment is available and whether the power plant is online. The HTF mass flow is non-zero during plant operation. When the power plant is inoperative, the HTF is modelled as stationary.

Fig. 13a displays the normalized power plant operating pattern with its corresponding modes (1 when the plant is online and 0 when it is offline). Fig. 13b displays the normalized curtailment pattern obtained from the curtailment model. The corresponding curtailment mode takes a value of 1 when curtailment is present and 0 when it is absent. Whenever curtailment is present, the thermal storage is being charged. While charging, a complete row of nodes is set to 165 °C to simulate the storage module heating elements. The exact row of nodes depends on the type of active mode presented in Fig. 12. While discharging, the temperature of the PCM drops below its melting point and the fuel temperature decreases until it reaches the ambient temperature (15 °C). Using these modes and the corresponding storage operation mode, the HTF outlet temperature is obtained from the storage model as displayed in Fig. 13c. This pattern is used to relate the total energy added to the sensible enthalpy of the fuel gas to the total energy added to the CCPP. By doing so, the impact of fuel preheating can be assessed and the total annual fuel savings can be quantified.

7. Fuel savings and financial feasibility

7.1. Fuel savings estimations

The annual fuel savings obtained by the thermal storage and fuel heating system are shown in Fig. 14 and Fig. 15. It can be seen that the fuel savings increase with wind penetration levels. Below a wind penetration of 10%, the fuel savings are negligible, a direct result of the low occurrence of curtailment. As expected, higher penetration levels (and therefore the available curtailment) lead to

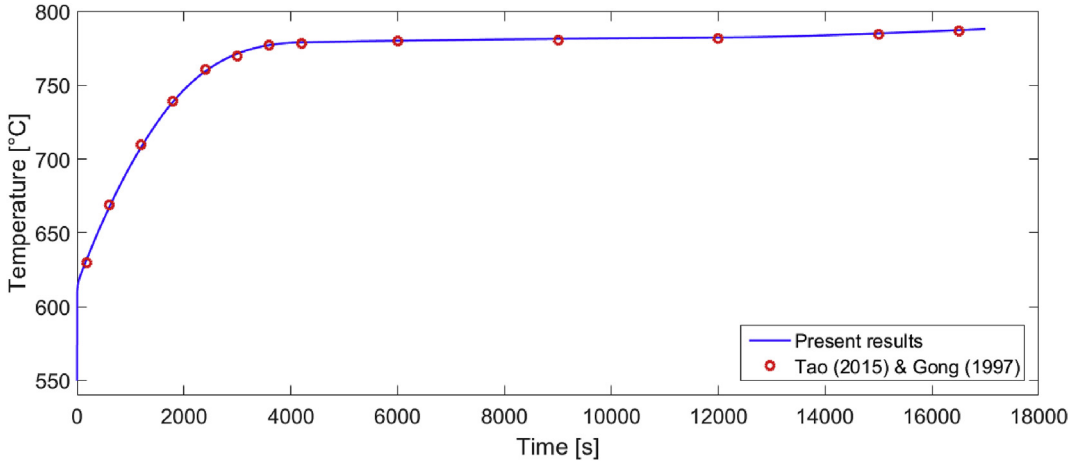

Fig. 10. Thermal storage model validation [13,35]].

Inputs	• SNSP limit • TCG limit • Annual demand pattern • Annual wind generation pattern	• Component data • Annual operating pattern	• Annual operating pattern • PCM properties • HTF properties • Storage module dimensions	
	Curtailment model		• Annual curtailment pattern	
		Combined-cycle model		• Annual performance summary (no curtailment utilization)
			Thermal storage model	• Annual fuel temperature pattern (curtailment utilization)
				Outputs

Fig. 11. Model integration N2 chart and the procedure.

Table 5
Simulation specifications and scenario settings.[14]

Parameter	Range/Value	Unit
Module baseline dimensions		
Length	20	[m]
Inner radius	0.05	[m]
Outer radius	0.10	[m]
HTF mass flow	0.007	[kg/s]
Number of modules	2732	[−]
Dimension scenarios		
Length	12.5–27.5 (2.5 increment)	[m]
Inner radius	0.02–0.08 (0.01 increment)	[m]
Curtailment scenarios		
Annual national demand	117,778	[GWh]
Wind penetration (percentage of demand)	10–50	[%]
SNSP limit (percentage of demand)	60	[%]
RR limit (percentage of maximum demand)	30	[%]

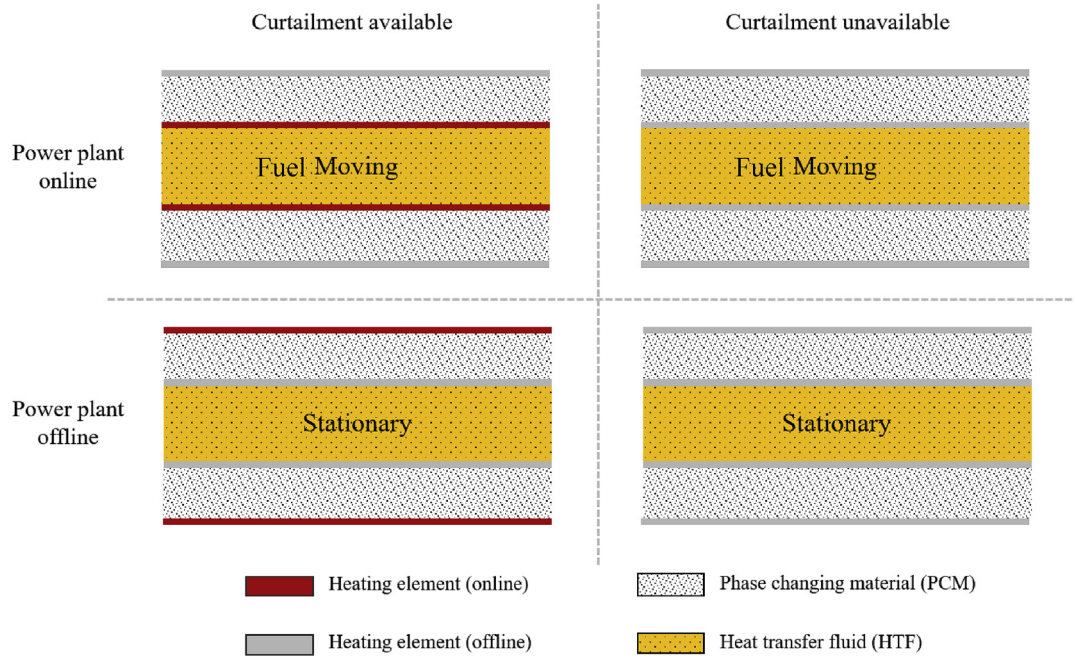

Fig. 12. Operation modes of the Thermal Storage and Heating System.

higher fuel savings. A significant increase occurs between 10% and 20% due to the relation between fuel consumption and wind penetration level. Secondly, decreasing the module length and inner radius leads to lower fuel savings, mainly due to the reduced heat capacity of the thermal storage system. However, it should be noted that their relationship is not linearly proportional. This is more apparent for higher wind penetration levels in which smaller thermal storage becoming more effective due to the increased frequency of curtailment. It can be seen from Fig. 15 that increasing the inner radius beyond 0.07 m has no effect on the fuel savings. It

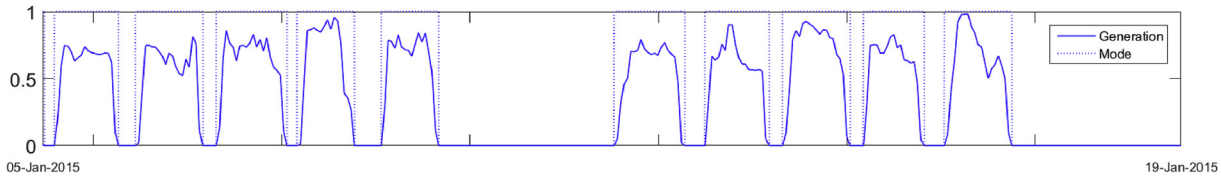

(a) Normalized CCPP generation and its corresponding operation mode (online/offline)

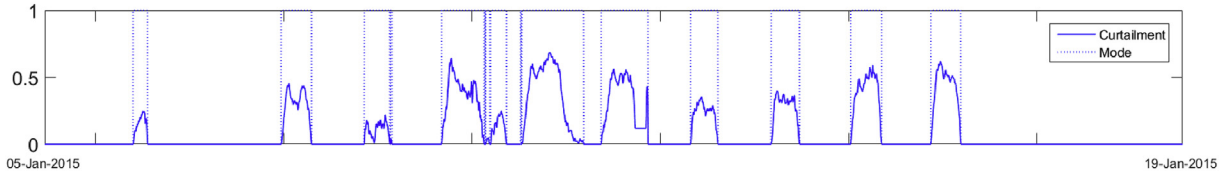

(b) Normalized wind curtailment and its corresponding operation mode (available /unavailable)

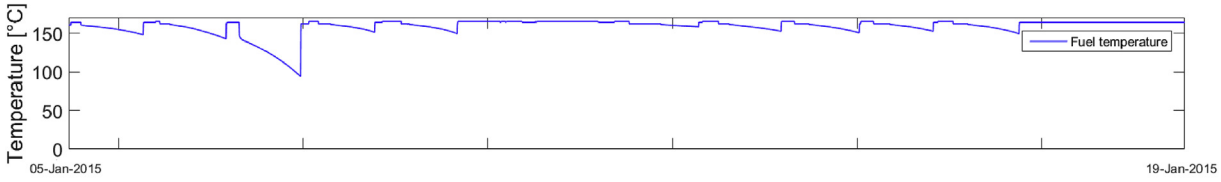

(c) The natural gas temperature at the storage outlet

Fig. 13. Illustrative result obtained from the numerical simulations.

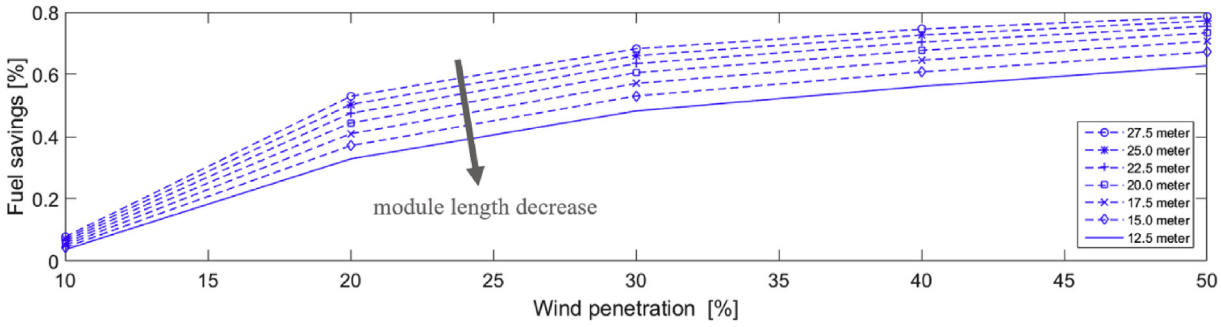

Fig. 14. Annual fuel savings for various thermal storage module lengths.

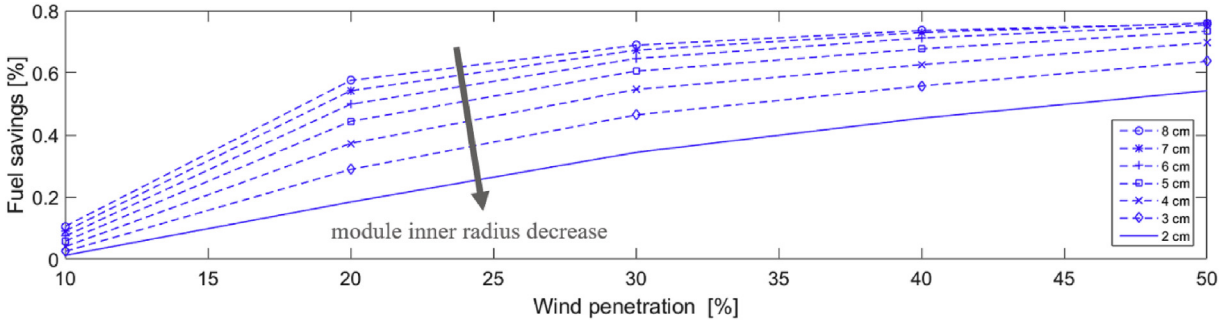

Fig. 15. Annual fuel savings for various thermal storage module inner radii.

should be noted that several of these modules are used in parallel. The maximum fuel savings that can be achieved from the proposed system is around 0.8% of total fuel, which corresponds to a saving of around 3600 tonnes CO_2 annually.

To address the financial feasibility of the project two metrics are used: the initial investment costs and project payback period. Both give an indication regarding the project's financial feasibility.

7.2. Financial benefits of the proposed concept

Two major financial benefits originate from the reduction in fuel consumption: fuel costs and CO_2 allowance costs. In 2015, the

Table 6
The financial cost estimates annually.

Profits			Investment Costs		
Parameter	Value	Unit	Parameter	Value	Unit
Input			Input		
Annual gas consumption	212, 030	[tonne]	No. of pipes	2732	[−]
Energy consumption	8,056,693	[GJ]	PCM vol./pipe	0.353	[m^3]
CO_2 emitted	451,191	[tonne]	PCM density (liquid)	1500	[kg/m^3]
Gas consumption savings	0.53	[%]	PCM latent heat of fusion	306	[kJ/kg·K]
Price of gas in NL	7.54	[EUR/GJ]	Price of PCM	2	[EUR/kg]
Price per gas, EU average	9.39	[EUR/GJ]	Price of PCM/kWhr	40	[EUR]
Price of CO2/tonne	5.24	[EUR]			
Output			Output		
Total fuel savings	321,970	[EUR]	Total PCM cost	2,896,705	[EUR]
CO_2 savings	12,530	[EUR]	Labour & Material costs	2,896,705	[EUR]
Total Profits	334,501	[EUR]	Total costs	5,793,411	[EUR]

average Dutch natural gas price was 7.54 EUR/GJ[15] and the price of CO_2/tonne was 5.24 EUR. Using the previously described methods and the numbers for annual fuel savings per storage size, the annual profits and investment costs can be calculated. It is assumed that the material and labour costs are the same as the thermal storage cost. An example of the balance sheet is presented in Table 6 for a storage module with a length of 15 m and an annual fuel savings percentage of 0.53% (30% wind penetration). On the profit side, one can see that a large portion of the savings comes from fuel savings rather than the saving on carbon allowances. However, it is expected that the price of the carbon will increase considerably in the future due to the global climate agreement and this would positively affect the feasibility of the proposed concept.

It should be noted that the gas price in the Netherlands is relatively low. Therefore its annual profit should be taken as being close to the lower boundary rather than a European average. Using the data presented in Table 6, the payback period for this scenario equals approximately 15.2 years. The inflation rate has been set to zero since the EUR inflation rates were close to zero for 2016. In July 2016 the Dutch inflation rate was even negative at a rate of −0.3%[16].

A cost estimation is performed with help of the cost of TES per kWh. This price is approximately 36 EUR/kWh [7,20]. Using this figure and the maximum available energy within the storage, its installation costs can be estimated. The total available energy is estimated by means of the specific enthalpy and total PCM mass. Using the previously described method and the numbers for annual fuel savings per storage size, the project's payback period is computed using eqn. (19).

$$PBP = \frac{C_I}{C_F + C_{CB}} \tag{19}$$

The investment costs and payback periods for some scenarios are presented in Fig. 16. As expected, the investment costs (shown in the legend between brackets) decrease for smaller TES dimensions due to a smaller storage. This figure shows that higher IRES penetration levels reduce the payback period. Furthermore, the figure shows that smaller dimensions of the storage unit are better from a payback time point of view. However, it should be noted that the cost model used for assessing the cost of the thermal storage system is rather simple and does not take into account several secondary costs. In reality, the secondary costs increase for smaller installations, thereby providing the economy of scale for larger installations.

8. Discussion and conclusions

A novel solution to store and utilize excess energy from intermittent renewable energy sources (IRES) in a combined cycle power plant (CCPP) is introduced. This excess energy is stored in the form of heat and is used to preheat natural gas during normal operation of the CCPP, resulting in a reduced fuel consumption. The techno-economic feasibility of this novel solution carried out using three coupled mathematical models.

The first model estimates the amount of curtailment available in the grid due to the variable and intermittent nature of the renewable energy production within the Netherlands. Representative values of the SNSP and reserve limits have been used to model the curtailment. The second model is that of a combined cycle power plant to model the performance of the power plant. This model was validated with the data available from the OEMs and the open literature. A recent and representative power plant operating in the Netherlands was used as a reference. The third model was that of the thermal storage system. The model was used to choose the working fluid and to calculate the dimensions of the thermal energy storage.

The three models were then combined to optimize the geometry of the thermal energy storage taking into account the curtailment and the power plant operating characteristics. It is found that the fuel savings are significantly dependent on the share of wind penetration in the grid and the capacity of the thermal storage. The proposed concept is financially feasible and the pay back period is not very long, between 5 and 10 years depending on the price of the fuel, the labour costs and the carbon cost. The cost model suggested that the main costs savings come from the reduction in the fuel consumption rather than the saving in the carbon budget.

Based on the simulations carried out using verified models, the following conclusions can be drawn:

- Wind curtailment can be used to preheat natural gas to a maximum temperature of 165 °C in combined-cycle power plants to reduce fuel consumption and CO_2 emissions.
- The proposed thermal energy storage system is suitable to fulfil the role of both energy storage and gas heater.

[15] Eurostat. 2016. Gas prices by type of user. [ONLINE] Available at: http://ec.europa.eu/eurostat. [Accessed: 03-08-2016].

[16] Centraal Bureau voor de Statistiek, \Inatie voor het eerst in bijna 30 jaar negatief." Available at: "https://www.cbs.nl/nl-nl/nieuws/2016/31/inflatie-voor-het-eerst-in-bijna-30-jaar-negatief". Accessed online: 04-08-2016.

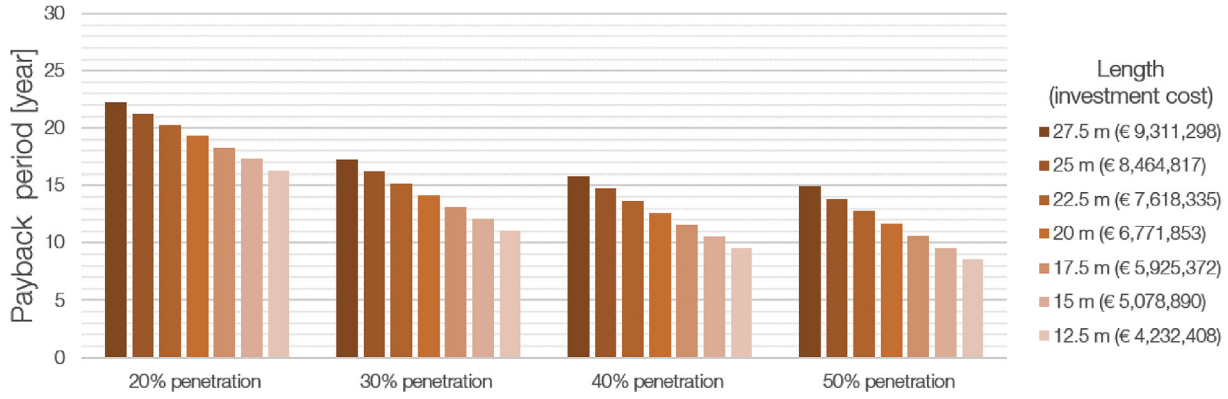

Fig. 16. Payback periods for various storage module lengths at a module inner radius of 5 cm. (in between the brackets in the legend the investment) for European gas prices.

- For the simulated scenarios, annual fuel savings up to 0.8% can be achieved. This translates into a reduction of approximately 3600 tonnes in CO_2 emissions.
- There is a strong coupling between the thermal storage capacity, national wind penetration level and annual fuel savings.
- High wind penetration levels increase the viability of the proposed concept and potential for a feasible business case.
- A large portion of the profits comes from fuel savings rather than from CO_2 costs with the current cost levels.
- The proposed concept paves the way to change the role of a combined-cycle power plant from being solely an energy provider to a contributor to energy storage and energy management.
- The overall thermal to electricity conversion efficiency is between 50% and 60%, comparatively higher than other contemporary energy storage methods.

Acknowledgements

The authors would like to express my appreciation to Theo Woudstra for his guidance and help with Cycle Tempo.

This research did not receive any specific grant from funding agencies in the public, commercial, or not-for-profit sectors.

References

[1] Arai J, Iba K, Funabashi T, Nakanishi Y, Koyanagi K, Yokoyama R. Power electronics and its applications to renewable energy in Japan'. Circ Sys Mag IEEE 2008;8(3):52–66.
[2] Barton JP, Infield DG. Energy storage and its use with intermittent renewable energy', *Energy Conversion*. IEEE Transactions on 2004;19(2):441–8.
[3] Beaudin M, Zareipour H, Schellenberglabe A, Rosehart W. Energy storage for mitigating the variability of renewable electricity sources: an updated review. Energy Sustain Dev. 2010;14(4):302–14.
[4] Bird L, Lew D, Milligan M, Carlini EM, Estanqueiro A, Flynn D, Gomez-Lazaro E, Holttinen H, Menemenlis N, Orths A, Eriksen PB, Smith JC, Soder L, Sorensen P, Altiparmakis A, Yasudam Y, Miller J. Wind and solar energy curtailment: a review of international experience. Renew Sustain Energy Rev 2016;65:577–86.
[5] Brouwer AS, van den Broek M, Seebregts A, Faaij A. Operational flexibility and economics of power plants in future low-carbon power systems. Appl Energy 2015;156:[107]–[128].
[6] Burke DJ, O'Malley MJ. Factors Influencing Wind Energy Curtailment. IEEE Trans Sustain Energy 2011;2(2):185–93.
[7] Chen H, Cong TN, Yang W, Tan C, Li Y, Ding Y. Progress in electrical energy storage system: a critical review. Prog Nat Sci 2009;19(3):291–312.
[8] Díaz-González F, Sumper A, Gomis-Bellmunt O, Villafáfila-Robles R. A review of energy storage technologies for wind power applications. Renew Sustain Energy Rev 2012;16(4):2154–71.
[9] Felderhoff M, Urbanczyk R, Peil S. Thermochemical heat storage for high-temperature applications–a review. Greenpeace 2013;3(2):113–23.
[10] Fleischer AS. Thermal energy storage using phase change materials: fundamentals and applications. Springer; 2015.
[11] Gardner P, Papadopoulos I. The limiting factors for wind integration. In: EWEA 2012 conference proceedings, copenhagen; 2012.
[12] Gil A, Medrano M, Martorell I, Lázaro A, Dolado P, Zalba B, Cabeza LF. State of the art on high temperature thermal energy storage for power generation. Part 1—concepts, materials and modellization. Renew Sustain Energy Rev 2010;14(1):31–55.
[13] Gong Z, Mujumdar AS. Finite-element analysis of cyclic heat transfer in a shell-and-tube latent heat energy storage exchanger. Appl Therm Eng 1997;17(6):583–91.
[14] Jacobsen HK, Schroder ST. Curtailment of renewable generation: economic optimality and incentives. Energy Pol 2012;49:663–75.
[15] Joos M, Staffell I. Short-term integration costs of variable renewable energy: wind curtailment and balancing in Britain and Germany. Renew Sustain Energy Rev 2018;86:45–65.
[16] Jun E, Kim W, Chang SH. The analysis of security cost for different energy sources. Appl Energy 2009;86(10):1894–901.
[17] Kamali S, Amraee T. Blackout prediction in interconnected electric energy systems considering generation re-dispatch and energy curtailment. Appl Energy 2017;187:50–61.
[18] Kehlhofer R, Hannemann F, Rukes B, Stirnimann F. Combined-cycle gas & steam turbine power plants. 2009.
[19] Kenisarin M, Mahkamov K. Solar energy storage using phase change materials. Renew Sustain Energy Rev 2007;11(9):1913–65.
[20] Kousksou T, Bruel P, Jamil A, El Rhafiki T, Zeraouli Y. Energy storage: applications and challenges. Sol Energy Mater Sol Cell 2014;120(Part A):59–80.
[21] Lacroix M. Numerical simulation of a shell-and-tube latent heat thermal energy storage unit. Sol Energy 1993;50(4):357–67.
[22] Lee R-T, Chiou W-Y. Finite-element analysis of phase-change problems using multilevel techniques. Numer Heat Tran 1995;27(3):277–90.
[23] Lund H. Large-scale integration of wind power into different energy systems. Energy 2005;30(13):2402–12.
[24] Luo G, Li Y, Tang W, Wei X. Wind curtailment of China's wind power operation: evolution, causes and solutions. Renew Sustain Energy Rev 2016;53:1190–201.
[25] Mc Garrigle EV, Deane JP, Leahy PG. How much wind energy will be curtailed on the 2020 Irish power system? Renew Energy 2013;55:544–53.
[26] McKenna E, Grünewald P, Thomson M. Going with the wind: temporal characteristics of potential wind curtailment in Ireland in 2020 and opportunities for demand response. Renew Power Generat IET 2015;9(1):66–77.
[27] Mehling H, Cabeza LF. Heat and cold storage with PCM. Springer; 2008.
[28] Niet T, Lyseng B, English J, Keller V, Palmer-Wilson K, Robertson B, Wild P, Rowe A. Valuing infrastructure investments to reduce curtailment. Energy Strat Rev. 2018;22:196–206.
[29] Patrick TM, Jurgen G, Price A, Droste-Franke B. Electrochemical energy storage for renewable sources and grid balancing. In: Garche PTM, editor. Electrochemical energy storage for renewable sources and grid balancing. Amsterdam: Elsevier; 2015.
[30] Pensini A, Rasmussen CN, Kempton W. Economic analysis of using excess renewable electricity to displace heating fuels. Appl Energy 2014;131:530–43.
[31] Ruester S, He X, Vasconcelos L, Glachant J. Electricity storage: how to facilitate its deployment and operation in the EU', *Think Final Report*. European University Institute; 2012.
[32] Sabera H, Moeini-Aghtaieb M, Ehsana M,, Fotuhi-Firuzabada M. A scenario-based planning framework for energy storage systems with the main goal of mitigating wind curtailment issue. Electri Power Energy Sys. 2019;104:414–22.
[33] Sharma SD, Sagara K. Latent heat storage materials and systems: a review. Int J Green Energy 2005;2(1):1–56.
[34] Steurer M, Fahl U, Voß A, Deane P. Curtailment: an option for cost-efficient integration of variable renewable generation. Europe's energy transition - insights for policy making. London: Academic Press; 2017. https://doi.org/10.1016/B978-0-12-809806-6.00036-5.

[35] Tao YB, He YL. Numerical study on performance enhancement of shell-and-tube latent heat storage unit. Int Commun Heat Mass Tran 2015;67:147–52.
[36] Testa F, Cosic A, Iraldo F. Determining factors of curtailment and purchasing energy related behaviours. J Clean Prod 2016;112:3810–9.
[37] Thakare K, Bhave AG. Review on latent heat storage and problems associated with phase change material. Int J Renew Energy Technol 2015;4:176–82.
[38] Ueckerdt F, Hirth L, Luderer G, Edenhofer O. System LCOE: what are the costs of variable renewables? Energy 2013;63:61–75.
[39] Waters CN, Zalasiewicz J, Summerhayes C, Barnosky AD, Poirier C, Gałuszka A, Cearreta A, Edgeworth M, Ellis EC, Ellis M, Jeandel C, Leinfelder R, McNeill JR, deB. Richter D, Steffen W, Syvitski J, Vidas D, Wagreich M, Williams M, Zhisheng A, Grinevald J, Odada E, Oreskes N, Wolfe AP. The Anthropocene is functionally and stratigraphically distinct from the Holocene. Science 2016;351:6269. https://doi.org/10.1126/science.aad2622.
[40] Yan X, Gu C, Li F, Ai Q. Cost-benefit comparison of different techniques for addressing wind curtailment. In: 9th international conference on applied energy, ICAE2017, 21-24 august 2017, cardiff, UK. *Energy procedia*, vol. 142; 2017. p. 1759–64.
[41] Zalba B, Marın JM, Cabeza LF, Mehling H. Review on thermal energy storage with phase change: materials, heat transfer analysis and applications. Appl Therm Eng 2003;23(3):251–83.
[42] Zhang Y, Faghri A. Heat transfer enhancement in latent heat thermal energy storage system by using the internally finned tube. Int J Heat Mass Tran 1996;39(15):3165–73.
43] Andoni Merlinda, Robu Valentin, Früh Wolf-Gerrit, Flynn David. Game-theoretic modeling of curtailment rules and network investments with distributed generation. Applied Energy 2017;201:174–87.